Mechanistic Studies of Methanol Oxidation to Formaldehyde on Isolated Vanadate Sites Supported on High Surface Area Zirconia

Jason L. Bronkema and Alexis T. Bell*

Chemical Sciences Division, Lawrence Berkeley National Laboratory and Department of Chemical Engineering, University of California, Berkeley, California 94720-1462

Received: November 20, 2007; In Final Form: February 6, 2008

The oxidation of methanol on both ZrO_2 and V/ZrO_2 was investigated using temperature-programmed experiments together with in situ infrared spectroscopy. Characterization of V/ZrO_2 after calcination by Raman spectroscopy and XANES shows that the vanadium is present as isolated VO_4 units in a distorted tetrahedral geometry. Methanol was found to adsorb dissociatively on both Zr−O−Zr and V−O−Zr species to create $Zr-OCH_3/Zr-OH$ and $V-OCH_3/Zr-OH$ pairs, respectively. Upon heating, CH_3OH and H_2O desorb initially from all samples. Above 423 K, surface formate species are detected while H_2 and CO are the main products formed on ZrO_2. Upon addition of vanadium, CH_2O production increases dramatically during temperature-programmed reaction. The absence of CH_2O during temperature-programmed desorption and oxidation experiments on V/ZrO_2 is likely due to rapid readsorption of the product onto the ZrO_2 support, leading to the formation of formate species and H_2. The apparent activation energy for V/ZrO_2 is 18 kcal/mol. The activities of isolated vanadate species supported on SiO_2, TiO_2, and ZrO_2 are compared and discussed.

Introduction

Isolated vanadate groups supported on metal oxides such as SiO_2, Al_2O_3, ZrO_2, and TiO_2 have been shown to be active for the selective oxidation of methanol to formaldehyde.[1−3] Characterization of the vanadate centers by multiple techniques has demonstrated that at low vanadium coverage the supported VO_4 species have a distorted tetrahedral geometry consisting of a single V═O bond and three V−O−M bonds (M = support metal), irrespective of support composition.[4−6] The composition of the support, however, has a large effect on catalyst activity. For example, it has been reported that the activity of VO_x/ZrO_2 is similar to VO_x/TiO_2, and 3 orders of magnitude higher than that of VO_x/SiO_2 under comparable reaction conditions.[1] The cause for this remarkable sensitivity to support composition is not well understood and, in particular, why ZrO_2 and TiO_2 should increase the activity for formaldehyde formation by such a large degree.

Attempts to understand the interactions of methanol with ZrO_2 and VO_x/ZrO_2 have been reported by several investigators. Dilara and Vohs have reported the results of temperature-programmed desorption (TPD) studies of methanol adsorbed on both the (100) and the (110) surfaces of cubic zirconia.[7] Methanol adsorbed dissociatively on both surfaces to form methoxide and hydroxyl species. The main product observed during TPD was methanol at temperatures below 700 K. It was also observed that approximately 25% of the methanol was converted to carbon monoxide, methane, and formaldehyde. However, formaldehyde was only observed on the $ZrO_2(110)$ surface, and this was attributed to steric factors leading to more accessible lattice oxygen. The authors proposed that bidentate dioxymethylene species are the reactive intermediates in the formation of formaldehyde. Narishige and Niwa have also conducted TPD studies of methanol adsorbed on ZrO_2 and have noted that surface carbonates and dioxymethylene species were present on the support.[8] During TPD, methanol was the major product with CO and CO_2 detected above 575 K. Formaldehyde was not observed to desorb from ZrO_2. Burcham and Wachs performed in situ infrared studies on a monolayer of VO_x supported on ZrO_2.[9] Methanol adsorbed to form $V-OCH_3$ species via reaction with V−O−Zr bonds. Transfer of a H atom from these species was taken to be the rate-limiting step in the formation of formaldehyde. Formate species were observed at higher temperatures due to the readsorption of formaldehyde formed during TPD.

The objective of this study was to investigate the mechanism of methanol oxidation to formaldehyde catalyzed by isolated vanadate species supported on zirconia, and to compare this to previous work in our group on isolated vanadates supported on silica and titania.[10,11] Raman spectroscopy and X-ray absorption near edge structure (XANES) were used to characterize the catalyst, and in situ infrared spectra acquired during temperature-programmed desorption (TPD), temperature-programmed oxidation (TPO), and temperature-programmed reaction (TPRx) were used to determine reaction intermediates leading to the formation of formaldehyde as well as other products observed in the gas phase. These studies show that, while zirconia will adsorb methanol and promote its oxidation to small amounts of formaldehyde, the introduction of isolated vanadate species onto the support greatly enhances the rate of formaldehyde formation.

Experimental Methods

A high surface area zirconia support was prepared by refluxing a 0.5 M solution of zirconyl chloride ($ZrO(NO_3)_2 \cdot 8H_2O$, 99.99%, Aldrich) for 10 days.[12] After the addition of NH_4OH to agglomerate the particles, the precipitate was recovered by vacuum filtration, washed with deionized water, and dried at 383 K for 12 h. The sample was calcined at 2 K/min to 873 K and held for 3 h, with dry air flowing at 100 cm^3/min.

* Author to whom correspondence should be addressed. E-mail: bell@cchem.berkeley.edu.

10.1021/jp7110692 CCC: $40.75
Published on Web 03/28/2008

Vanadium oxide was deposited onto the zirconia by chemical vapor deposition. Vanadium acetylacetonate [$VO(acac)_2$] (Aldrich, 98%) and ZrO_2 were mixed in a mortar and pestle and then placed inside a quartz reactor. The mixture was heated to 513 K at 5 K min^{-1} in N_2 flowing at 30 cm^3 min^{-1} and then held at this temperature for 3 h to ensure complete reaction. The gas flow was changed to zero-grade air flowing at 100 cm^3 min^{-1} and the material was calcined at 773 K for 17 h. The loading of V was determined to be 1.9 wt % by ICP.

The BET surface area of the sample was measured using a Micromeritics Autosorb-1 instrument. Prior to carrying out N_2 adsorption/desorption measurements each sample (50 mg) was outgassed for 16 h at 393 K. By using the five-point Brunauer−Emmett−Teller (BET) method, the surface area was calculated to be 84 m^2/g. On the basis of this surface area, the surface density of vanadium is 2.0 V/nm^2, which is well below the level of 7 V/nm^2 at which isolated vanadate groups begin to form polyvanadate species and V_2O_5 crystallites.[13]

Infrared spectra were recorded using a Thermo-Nicolet NEXUS 670 FT-IR equipped with an MCT-A detector. Spectra were recorded with a resolution of 2 cm^{-1}, with 32 scans averaged for each spectrum. Samples (40 mg) were pressed into 20 mm diameter pellets at 10 000 psi and placed within a low dead volume in situ infrared cell, containing CaF_2 windows, capable of reaching temperatures up to 773 K.

Pulsed-adsorption of methanol was performed in order to determine the amount of methanol adsorbed on ZrO_2 and V/ZrO_2. For these experiments, ~40 mg of catalyst was placed into a quartz microreactor. The reactor was flushed with ultrahigh pressure (UHP) He and then heated to 323 K. Methanol was introduced by flowing UHP He through a methanol-filled bubbler maintained at 293 K. The methanol/He mixture was passed through a 6 way valve to which was attached a 0.49 cm^3 dosing volume held at 338 K. Under these conditions, the amount of methanol in each pulse was 2.28 μmol. The exit stream from the microreactor was monitored by a mass spectrometer to quantify the methanol leaving the reactor during each pulse. Pulses of methanol were supplied to the reactor until three successive pulses of equal size were observed. The total amount of methanol adsorbed, N_{MeOH}, was calculated by the equation:

$$N_{MeOH} = N^0_{MeOH}(nA_{max} - \sum_{i=1}^{n} A_i)/nA_{max} \quad (1)$$

where N^0_{MeOH} is the amount of methanol in each pulse, n is the total number of pulses, A_{max} is the average area of the three successive pulses measured at the point of adsorbent saturation, and A_i is the area of the ith pulse of methanol observed by the mass spectrum.

Temperature-programmed desorption, oxidation, and reaction experiments (TPD, TPO, and TPRx, respectively) were carried out in both the infrared cell and a quartz microreactor. Methanol was adsorbed from a mixture of 4% methanol in helium flowing at 30 cm^3 min^{-1}. A catalyst sample weighing ~40 mg was exposed to the methanol-containing gas at 323 K for 3 min. A short exposure time was used to minimize the loss of vanadium from the catalyst.[10] Following adsorption, the reactor was purged with a flow of 100 cm^3 min^{-1} of He for at least 45 min in order to remove any residual gas-phase methanol. For TPD experiments, the samples were then heated in He flowing at 30 cm^3 min^{-1}, whereas for TPO experiments, the samples were heated in a 5% O_2/He mixture flowing at 30 cm^3 min^{-1}. For TPRx experiments, the samples were exposed to a mixture of 6% MeOH/12% O_2/He flowing at 30 cm^3 min^{-1}. For all three types of experiment, the temperature was ramped from 323 to 773 K at 4 K/min. Infrared spectra were collected every 75 s in order to obtain a scan every 5 K. The effluent from both the infrared cell and the microreactor was analyzed by an MKS Mini-Lab quadrupole mass spectrometer. Data were collected for 27 masses every 7.5 s. Response factors and fragmentation patterns were determined for H_2, H_2O, O_2, CO, CO_2, CH_3OH, CH_2O, CH_3OCH_3, and CH_4 relative to the He signal, which was used as an internal standard, and the values were adjusted to account for the isotopic abundance of both carbon and oxygen. Because the fragmentation pattern of methanol, formaldehyde, oxygen, and carbon monoxide produce overlapping peaks in the range of m/e = 28−33, a matrix deconvolution procedure was used to quantify the gas-phase contributions of each species. After analysis, the data were smoothed using adjacent-averaging of 15 points.

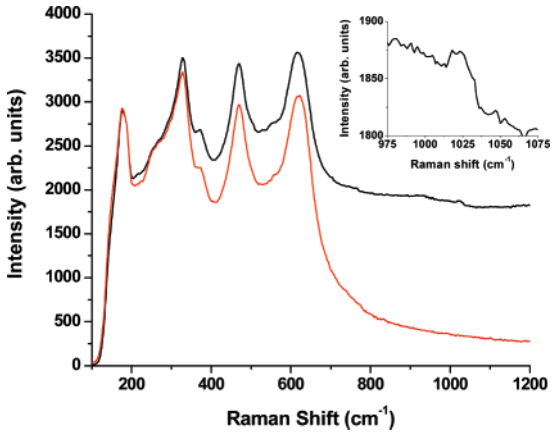

Figure 1. Raman spectrum of V/ZrO_2 (black) and ZrO_2 (red) after dehydration in dry air at 773 K for 2 h. Inset in Raman plot shows the difference between V/ZrO_2 and ZrO_2 in the region between 975 and 1075 cm^{-1}.

X-ray absorption (XAS) measurements were performed at the Stanford Synchrotron Radiation Laboratory (SSRL) on beam line 2−3. These measurements were performed at the vanadium K-edge. The edge energy for each sample was determined as the first inflection point of the main peak in the spectrum, and the edge energy of the vanadium foil was set to 5465 eV. The optimal sample amount was calculated on the basis of the weight fraction of all atomic species to obtain an absorbance of ~2.5, with boron nitride added if necessary to make a stable pellet. Samples were placed in a controlled-atmosphere cell that allowed for heating up to 823 K in the presence of flowing gas.[14] The V/ZrO_2 sample was pretreated for 2 h at 773 K in 10% O_2/He flowing at 30 cm^3 min^{-1}. After the pretreatment was completed, the cell was evacuated to 6×10^{-4} Pa and cooled to 77 K before the XAS data were collected.

The software program IFEFFIT, along with its complementary GUIs Athena and Artemis, was used for the data analysis.[15,16] First, a linear pre-edge was subtracted from the data, fit to the range of −150 to −75 eV relative to the edge energy. Then a quadratic polynomial fit to the range of 100 to 300 eV, relative to the edge energy, was used to determine the postedge line. The difference between the two lines at the edge energy was set to 1 to normalize the data.

Results and Discussion

Catalyst Characterization. Raman spectra of both ZrO_2 and V/ZrO_2 are shown in Figure 1. For ZrO_2, there are peaks at 178, 256, 328, 373, 469, and 618 cm^{-1}. The peak at 256 cm^{-1}

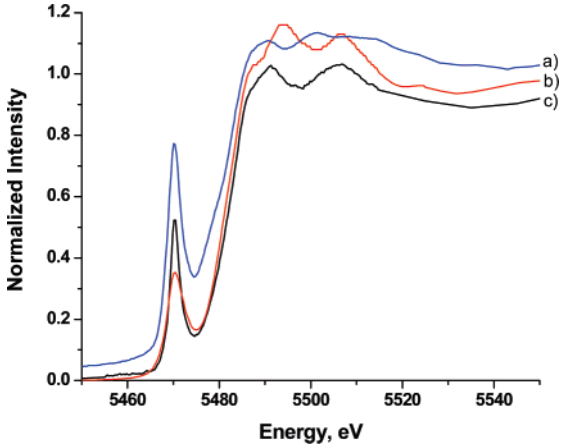

Figure 2. Normalized XANES spectra of (a) $NaVO_3$, (b) V_2O_5, (c) V/ZrO_2.

is characteristic of tetragonal zirconia, whereas the peaks at 178, 328, and 373 cm^{-1} are characteristic of monoclinic zirconia. This shows that both crystal phases are present at the surface of the zirconia. After the addition of vanadium, a broad band is observed at 1025 cm^{-1} because of the symmetric stretch of the vanadyl bond. While the frequency of this band is lower than that reported previously, 1041−1033 cm^{-1}, this difference can be explained by the low vanadia surface density of the sample used in these studies.[17] No features are observed at 995 cm^{-1} or lower wavelengths, indicating the absence of V_2O_5.

X-ray absorption experiments were performed to identify the oxidation state and local structure of the vanadium centers dispersed on the zirconia. Figure 2 shows the normalized XANES spectrum of V/ZrO_2 after calcination. XANES spectra for $NaVO_3$ and V_2O_5 are also shown for reference. For calcined V/ZrO_2, the edge energy is 5484.0 eV. This value lies between the edge energies for V^{5+} in $NaVO_3$ at 5483.5 eV and V_2O_5 at 5484.8 eV, strongly suggesting that after calcination the oxidation state of the V is +5.

Vanadium in $NaVO_3$ has tetrahedral symmetry, whereas the V in V_2O_5 has square planar or distorted octahedral symmetry. The size of the pre-edge peak at 5470 eV can be used to determine the coordination of the vanadium atom if the standards and samples have the same formal oxidation state and the same ligands in the first coordination shell. Since the pre-edge peak is due to electron transitions from the vanadium 1s to 3d level,[18] which are spin forbidden, the intensity of this peak should be weak. However, when the geometry around the vanadium atom becomes noncentrosymmetric, mixing between the oxygen 2p and the vanadium 3d levels can occur, leading to an increase in the observed intensity. This means that a purely octahedral geometry will have almost no pre-edge feature, whereas tetrahedrally coordinated V will have a large pre-edge feature. On the basis of a comparison to the geometry of the standards, the calcined V/ZrO_2 has a distorted tetrahedral geometry similar to that of $NaVO_3$.

Interactions of Methanol with ZrO_2. Figure 3a shows that upon adsorption of methanol on zirconia at 323 K, new infrared bands are observed at 1444, 1465, 1610, and 2812 cm^{-1}, as well as broad peaks centered at 2925 and 3300 cm^{-1}. The bands at 1465, 2812, and 2925 cm^{-1} are attributable to methoxide species formed by dissociative adsorption of methanol across Zr−O−Zr bonds to produce both the $Zr-OCH_3$ and the Zr−OH species.[19,20] The large increase in the number of surface Zr−OH groups also leads to hydrogen bonding between neighboring surface hydroxyl groups, as evidenced by the

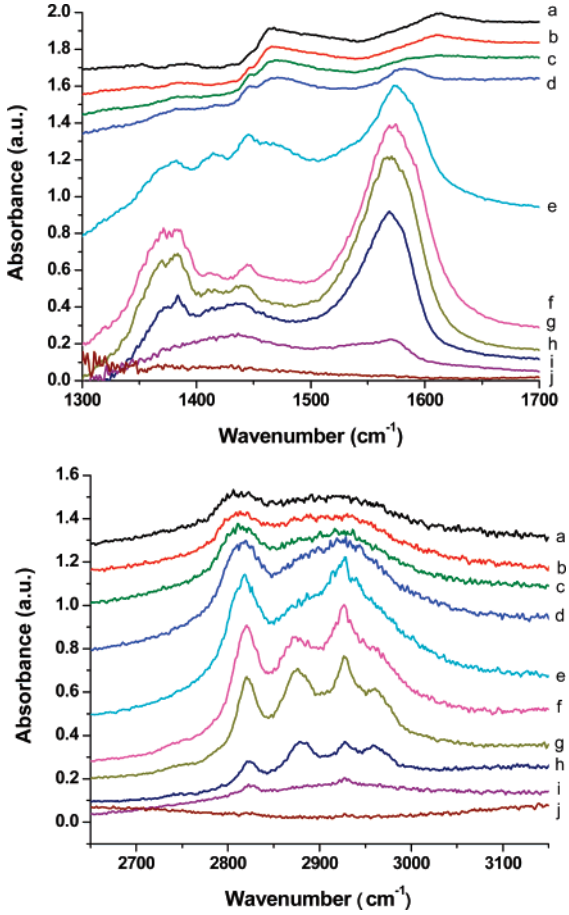

Figure 3. Low and high wavenumber infrared spectra of ZrO_2 taken during TPD of adsorbed methanol. Flow rate of He, −30 cm^3 min^{-1}. (a) 323, (b) 373, (c) 423, (d) 473, (e) 523, (f) 573, (g) 623, (h) 673, (i) 723, (j) 773 K.

TABLE 1: Tabulated Assignment of All Infrared Bands Detected on the Surface of Anatase and V/ZrO_2 under Experimental Conditions Where a Range Is Given for Each Assignment Because of the Shift in the Peak Positions at Different Temperatures or Surface Coverage

	Zr	V
δ C−H ($-OCH_3$)	1445, 1465	1470−1473
δ_{sym} O−C−O (CHOO)	1380−1384	1373−1377
δ_{asym} O−C−O (CHOO)	1569−1582	1564−1578
ν_{sym} C−H ($-OCH_3$)	2812−2820	2822−2832
ν_{asym} C−H ($-OCH_3$)	2925−2928	2929−2932
ν C−H (CHOO)	2873−2878	2880−2884
	2958−2961	2962−2965

formation of a broad band at 3300 cm^{-1} and the loss of the bands at 3675 and 3765 cm^{-1}, which were observed for the calcined sample and have been previously assigned to isolated hydroxyl groups.[9] The band at 1610 cm^{-1} is attributed to the formation of water on the surface of the catalyst. These band assignments, along with other surface species detected in the temperature-programmed experiments on both ZrO_2 and V/ZrO_2 are listed in Table 1.

Infrared spectra recorded during the TPD of methanol adsorbed on ZrO_2 are shown in Figure 3. From 323 to 473 K, there is very little difference in the infrared bands on the surface. The bands seen in Figure 3a−d are very broad and become better defined at high temperatures. This pattern is associated with the very high absorbance of the sample in the presence of methanol. As the concentration of adsorbed species decreased, the sample absorbance decreased and the quality of the data improved. At temperatures above 523 K, new bands appear at

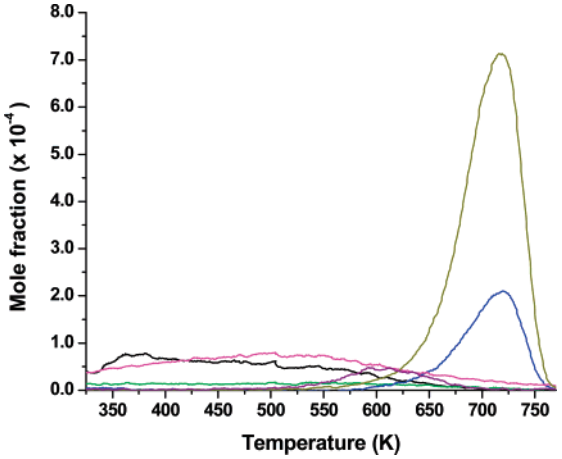

Figure 4. Gas-phase concentrations observed during TPD of methanol adsorbed on ZrO_2. Flow rate of He, −30 cm^3 min^{-1}. Methanol, black; formaldehyde, green; water, pink; carbon monoxide, blue; hydrogen, gold; dimethylether, purple.

1383 and 1574 cm^{-1} that can be assigned to surface formate species on zirconia.[7,20] The intensity of these bands increased significantly above 573 K, and two new bands appeared at 2873 and 2960 cm^{-1}, which are also attributed to formate species.[20] The decrease in intensity of the formate bands between 623 and 723 K is paralleled by desorption of CO and H_2, suggesting that these products are formed by the decomposition of formate species. The DME formed under these conditions is likely due to the reaction of two neighboring methoxide groups on the zirconia surface, thereby regenerating surface Zr−O−Zr bonds.

The composition of gas-phase species produced during TPD is presented in Figure 4. At temperatures below 500 K, the only products desorbed are methanol and water in approximately equal amounts, along with a small amount of formaldehyde. Above 500 K, there is a small peak due to DME centered at 600 K. Hydrogen desorbs from the catalyst above 575 K, along with CO. Both products reach a maximum at 725 K. Quantification of all gas-phase species was done by integration of the TPD peaks, and the results are presented in Table 2. It is noted that over three molecules of H_2 desorb per molecule of CO, which is higher than the 2:1 ratio expected based on the H/C ratio in the adsorbed methanol. The H/C ratio for all desorbed products is 5.5 and the O/C ratio is 1.4. These values are larger than 4 and 1, respectively, that would be predicted on the basis of the assumption that all products are formed exclusively from the methanol adsorbed on the catalyst. It is likely that hydroxyl groups present on the surface of ZrO_2 after calcination contribute oxygen and hydrogen to the products. It is also possible that the increased ratios are due to some residual carbonaceous species on the catalyst surface; however, the infrared spectra at 773 K do not show any evidence for surface formate or carbonate species.

Infrared spectra recorded during the TPO of methanol adsorbed on ZrO_2 are shown in Figure 5, and the composition of gas-phase species produced during this process is presented in Figure 6. The infrared spectra in Figure 5 are nearly identical to those in Figure 3 during the TPD, suggesting that the presence of gas-phase oxygen makes little difference in the reaction of adsorbed methoxide species on the surface. However, there are some small changes in the gas-phase species as seen in Figure 6. Again methanol, water, and formaldehyde are the only products below 500 K, and the DME peak is at the same position as previously located; however, there is only about half as much DME as formed during TPD. This is likely due to the oxidation of DME to CO_x and H_2O in the presence of gas-phase oxygen.

The presence of gas-phase oxygen leads to a shift in the CO and H_2 peaks to 635 K and the appearance of a small CO_2 peak at 650 K. The CO_2 peak is likely due to the combustion of CO in the presence of oxygen, since it was not detected during TPD. The total amount of CO and CO_2 increases from 0.69 to 0.97 atoms/nm^2, suggesting that gas-phase oxygen increases the combustion of surface methoxide and formate species. A new H_2O peak centered at 680 K also appears. This latter feature is due most likely to combustion of some of the desorbing H_2, since the total amount of hydrogen desorbed decreased by 1.2 atoms/nm^2.

Attempts were made to record infrared spectra during the TPRx of methanol adsorbed on ZrO_2. However, infrared spectra could not be obtained because of complete absorption of the infrared beam by gas-phase methanol under these conditions. The composition of gas-phase species produced during TPRx is presented in Figure 7. Initially, H_2O is the only product formed, with trace amounts of CH_2O and CO_2 observed above 400 K. As the temperature increases above 450 K, CO, H_2, and DME are also formed. The conversion remains below 3% until 575 K, above which the combustion of methanol increases rapidly. At all temperatures, the main product is water, with hydrogen being the second most abundant species below 750 K. The next most abundant products are CO and CO_2, and to a lesser extent DME. Above 700 K, the production of DME passes through a maximum as this product begins to combust, resulting in a concurrent increase in the formation of CO and CO_2. The combustion of H_2, as well as DME, above 700 K contributes to the observed increase in the formation of H_2O.

Interactions of Methanol with V/ZrO_2. Infrared spectra recorded after the adsorption of methanol adsorbed on V/ZrO_2 are shown in Figure 8a. New infrared bands are observed at 1473, 2823, and 2930 cm^{-1}, and a broad peak is centered at 3400 cm^{-1}. The bands at 1473, 2823, and 2930 cm^{-1} are very similar to those previously attributed to $V-OCH_3$ species on ZrO_2 supports and have therefore been attributed to $V-OCH_3$ species.[9] Because of the broad nature of these peaks and the similar position of methoxide species on both vanadium and zirconia, it is possible that methoxide species are present on the zirconia under these conditions as well. Upon adsorption, the isolated Zr−OH bands at 3675 and 3765 cm^{-1} are removed, and a broad band at 3400 cm^{-1} is observed. The latter feature is due to hydrogen bonding between surface Zr−OH groups. Also notable is the increased sharpness of the C−H stretching bands compared with those observed for ZrO_2 (see Figure 3). This change is due to a weaker absorption of the infrared beam after the addition of vanadium to the zirconia support.

Infrared spectra recorded during the TPD of methanol adsorbed on V/ZrO_2 are shown in Figure 8. From 323 to 423 K, there is little difference in the infrared bands on the surface. At temperatures above 473 K, new bands appear at 1375 and 1575 cm^{-1}, which are assigned to formate species formed on the surface of zirconia. The intensity of these bands increases as the temperature is raised to 623 K, and a new band appears at 2884 cm^{-1} when the surface formate concentration is high. This band has been previously attributed to surface formate species.[20,21]

The gas-phase species during the TPD of methanol on V/ZrO_2 are shown in Figure 9. It is observed that methanol and water are the major species desorbing below 400 K, together with a small amount of formaldehyde. This pattern is similar to that observed for ZrO_2 (see Figure 4). Above 400 K, H_2 is first observed, which is 125 K lower than on ZrO_2 as shown in Figure 4. CO, DME, and small amounts of CO_2 are observed at

TABLE 2: Total Amounts of Each Product Released into the Gas Phase during TPD and TPO of Methanol Adsorbed on ZrO_2 and V/ZrO_2[a]

		CH_3OH	CH_2O	CO	CO_2	H_2O	H_2	CH_4	DME	total C	total H	total O	MeOH adsorbed
ZrO_2	TPD	0.80	0.24	0.69	0	1.08	2.37	0	0.23	2.18	11.94	3.04	1.96
ZrO_2	TPO	0.77	0.31	0.86	0.11	1.53	1.11	0	0.13	2.32	9.79	3.83	1.99
$V-ZrO_2$	TPD	1.01	0.31	0.97	0.06	1.22	1.84	0.17	0.04	2.59	11.66	3.66	2.22
$V-ZrO_2$	TPO	0.93	0.34	0.86	0.33	2.87	0.94	0	0	2.46	12.02	5.66	2.08

[a]Total amounts of carbon, hydrogen, and oxygen removed from the surface based on the species observed in the gas phase. The right-hand-most column is the amount of methanol adsorbed on the surface based on the methanol pulsing experiments. All quantities are in atoms/nm^2.

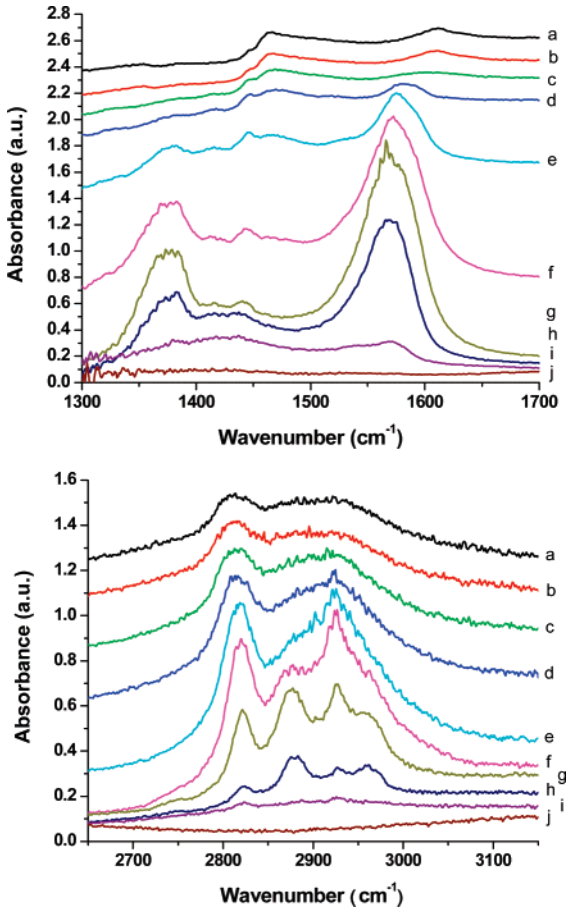

Figure 5. Low and high wavenumber infrared spectra of ZrO_2 taken during TPO of adsorbed methanol. Flow rate of 5% O_2/He, −30 cm^3 min^{-1}. (a) 323, (b) 373, (c) 423, (d) 473, (e) 523, (f) 573, (g) 623, (h) 673, (i) 723,(j) 773 K.

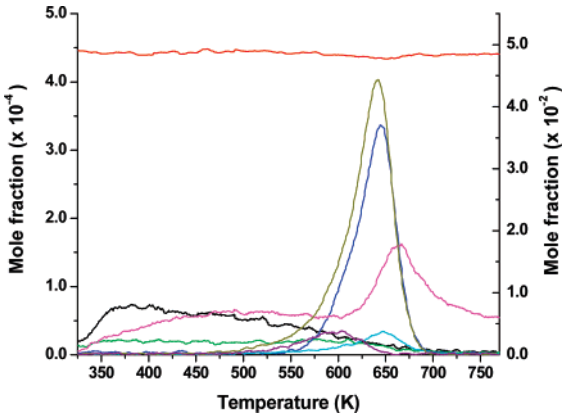

Figure 6. Gas-phase concentrations observed during TPO of methanol adsorbed on ZrO_2. Flow rate of 5% O_2/He, −30 cm^3 min^{-1}. Left axis: methanol black; formaldehyde green; water pink, carbon monoxide blue; carbon dioxide, light blue; hydrogen, gold; dimethylether, purple. Right axis: oxygen, red.

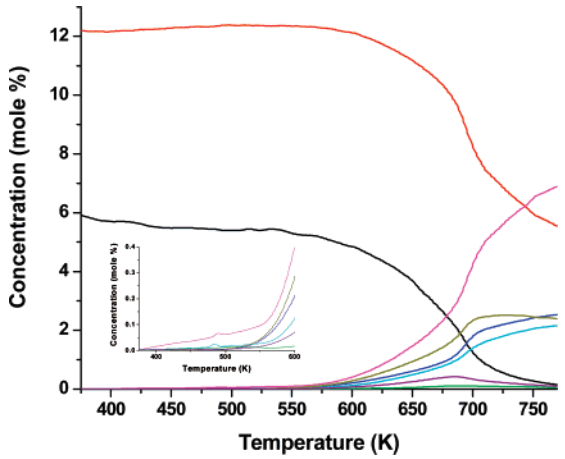

Figure 7. Gas-phase concentrations observed during TPRx of ZrO_2 in 6%MeOH/12%O_2/He flowing at 30 cm^3 min^{-1}. Methanol, black; oxygen, red; formaldehyde, green; water, pink; carbon monoxide, blue; carbon dioxide, light blue; hydrogen, gold; dimethylether, purple.

temperatures above 525 K, with the CO and H_2 both reaching a maximum at 615 K. A small methane peak starting at 525 K and reaching a maximum at 630 K is also detected. This peak was not observed on ZrO_2 under any conditions. The methane is most likely due to the reduction of $V-OCH_3$ species by gas-phase H_2, leaving a $V-OH$ species on the surface of the catalyst.

It is noted that the TPD spectrum for methanol adsorbed on V/ZrO_2 looks very similar to that observed during the TPO of methanol adsorbed on ZrO_2. The absence of a formaldehyde peak may be due to the rapid adsorption of newly formed CH_2O on the surface of ZrO_2.[21] The adsorption of formaldehyde on a $Zr-OH$ species would lead to the formation of a surface formate species and hydrogen. The formate species can then undergo further decomposition to produce CO and restore the $Zr-OH$ species. This would explain both the increased concentration of formate species below 523 K detected on the surface by infrared spectroscopy, as well as the shoulder in the H_2 desorption peak below 523 K. The O/C ratio in the products desorbed from V/ZrO_2 is 1.4, the same as that found for products desorbed from ZrO_2.

Infrared spectra recorded during the TPO of methanol adsorbed on V/ZrO_2 are shown in Figure 10. The infrared spectra during TPO are very similar to those observed in Figure 8 during TPD. One difference is an increase in the size of the formate peak detected between 523 and 673 K, along with an increase in the width of the formate bands. These observations suggest that there are likely multiple types of formate species present on the catalyst surface. Dilara and Vohs have suggested that formate species might bridge one zirconium atom or two.[7] The formate bands are also removed by 673 K, whereas formates were still present at 723 K during TPD. The other difference is the appearance of a new band at 2965 cm^{-1} between 523 and 573 K, which is likely due to formate species, and it is only detected here because of the increased concentration of formate species on the catalyst surface under TPO conditions.

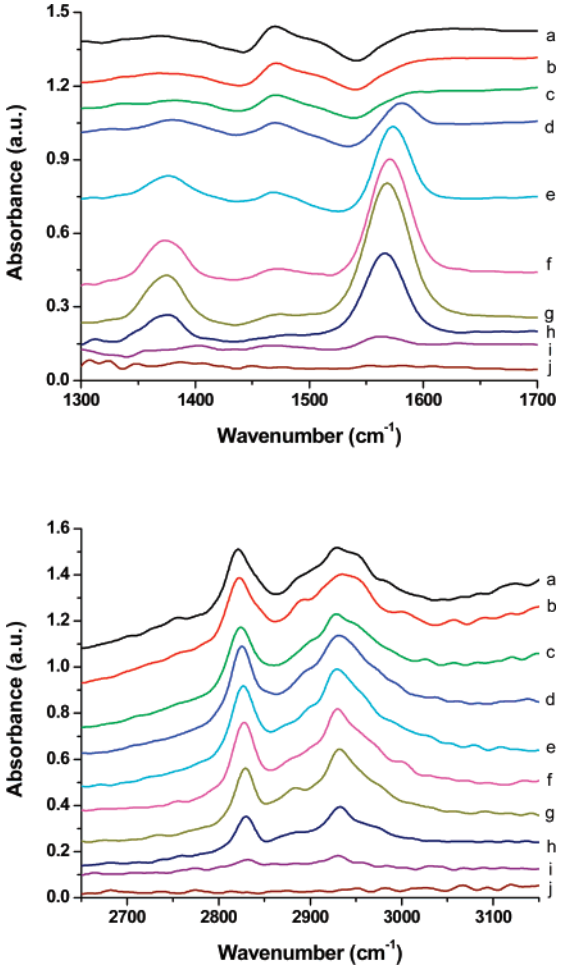

Figure 8. Low and high wavenumber infrared spectra of V/ZrO_2 taken during TPD of adsorbed methanol. Flow rate of He, −30 cm^3 min^{-1}. (a) 323, (b) 373, (c) 423, (d) 473, (e) 523, (f) 573, (g) 623, (h) 673, (i) 723, (j) 773 K.

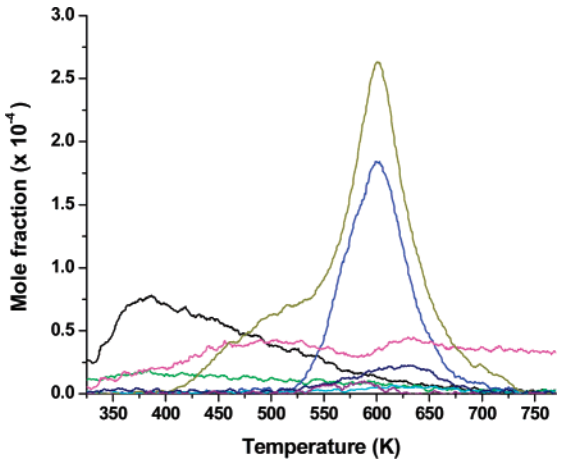

Figure 9. Gas-phase concentrations observed during TPD of methanol adsorbed on V/ZrO_2. Flow rate of He, −30 cm^3 min^{-1}. Methanol, black; formaldehyde, green; water, pink; carbon monoxide, blue; carbon dioxide, light blue; hydrogen, gold; methane, navy; dimethylether, purple.

The composition of gas-phase species produced during TPO is shown in Figure 11. Again methanol, water, and formaldehyde are the only species detected initially. Above 400 K, H_2 starts to desorb, reaching a maximum at 510 K. The CO peak reaches a maximum at 540 K. Also present are a large H_2O peak centered at 525 K and a CO_2 peak centered at 550 K. Finally,

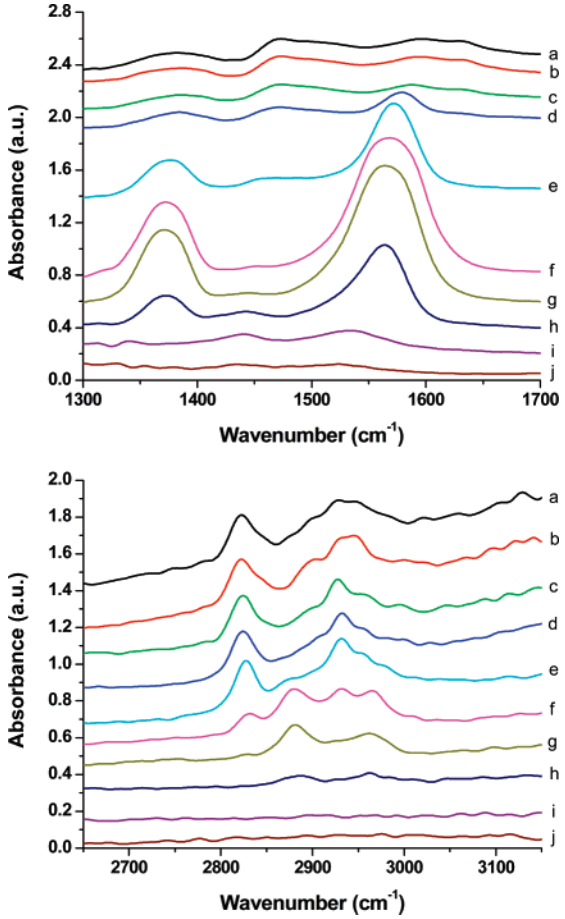

Figure 10. Low and high wavenumber infrared spectra of V/ZrO_2 taken during TPO of adsorbed methanol. Flow rate of 5% O_2/He, −30 cm^3 min^{-1}. (a) 323, (b) 373, (c) 423, (d) 473, (e) 523, (f) 573, (g) 623, (h) 673, (i) 723, (j) 773 K.

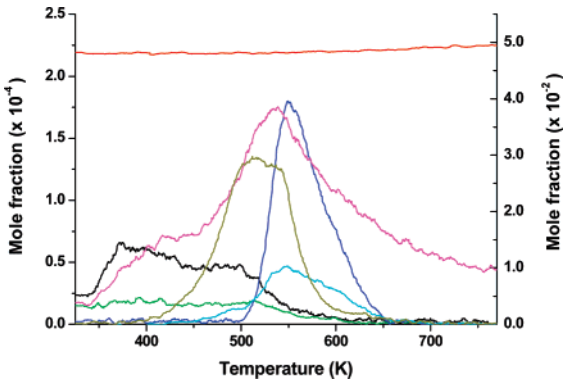

Figure 11. Gas-phase concentrations observed during TPO of methanol adsorbed on V/ZrO_2. Flow rate of 5% O_2/He, −30 cm^3 min^{-1}. Left axis: methanol, black; formaldehyde, green; water, pink; carbon monoxide, blue; carbon dioxide, light blue; hydrogen, gold. Right axis: oxygen, red.

no DME was detected in the gas phase under TPO conditions, likely because DME is rapidly oxidized to CO_x and H_2O.

One major difference observed during TPO on V/ZrO_2 is that CO and H_2 do not desorb simultaneously. Another difference is the absence of an increase in the formaldehyde production. Finally, the surface formate species are produced in high quantities at lower temperatures than in other experiments. These observations can be explained as follows. The formation of formaldehyde is envisioned to form from $V-OCH_3$ in a manner very similar to that observed in similar experiments conducted with V/SiO_2 and V/TiO_2.[10,11] However, in this case, the

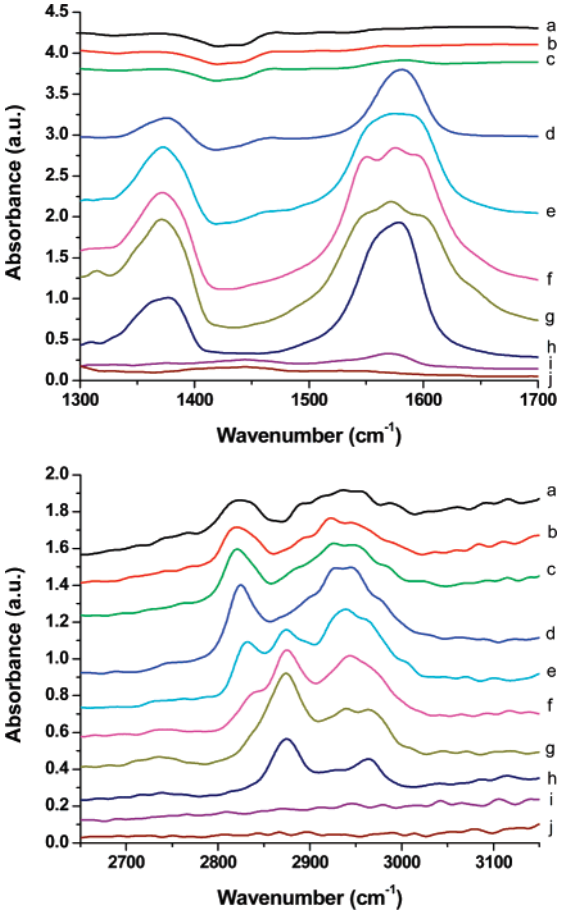

Figure 12. Low and high wavenumber infrared spectra of V/ZrO_2 taken during TPRx in 5%MeOH/12%O_2/He flowing at 30 cm^3 min^{-1}. (a) 373, (b) 423, (c) 473, (d) 523, (e) 573, (f) 623, (g) 673, (h) 723, (i) 773 K.

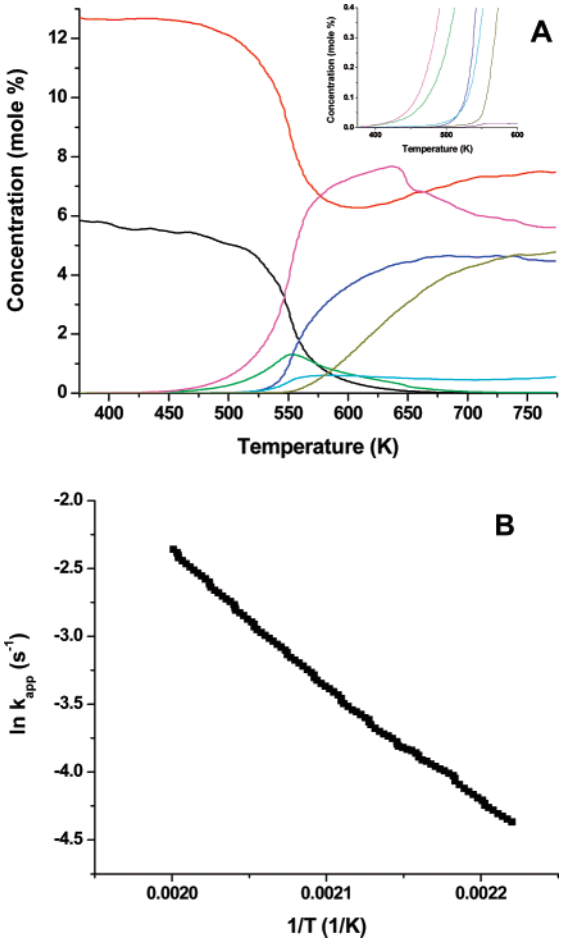

Figure 13. (A) Gas-phase concentrations observed during TPRx of V/ZrO_2 in 6% MeOH/12% O_2/He flowing at 30 cm^3 min^{-1}. Methanol, black; oxygen, red; formaldehyde, green; water, pink; carbon monoxide, blue; carbon dioxide, light blue; hydrogen, gold. (B) Arrhenius plot for the formaldehyde formation.

formaldehyde reacts rapidly with Zr−OH groups to form a surface formate species and H_2. As the temperature is increased, the surface formate species decomposes to form CO_x. This scheme likely happens to a limited extent on V/ZrO_2 during TPD conditions, which would explain the low temperature shoulder on the H_2 desorption peak. The increase in the amount of H_2O and CO_2 formed during TPO is likely due to the combustion of H_2 and CO respectively with gas-phase oxygen. This reaction likely occurs at the vanadium centers, since the amount of CO_2 and H_2O is highest when vanadium is present.

Infrared spectra recorded during the TPRx of methanol adsorbed on ZrO_2 are shown in Figure 12. The infrared bands during TPRx are very similar to the bands seen during TPO (see Figure 10). In this case, however, the formate bands at 1360 and 1575 cm^{-1} are broader, and the band at 1575 cm^{-1} has at least three distinct components at 623 and 673 K. This means that there are multiple species present on the catalyst surface, probably formates in monodentate and bidentate orientation, and possibly bridging both vanadium and zirconium atoms.

The composition of gas-phase species produced during TPRx is presented in Figure 13A. One major difference between these spectra and those shown in Figure 7 for ZrO_2 is the presence of a large formaldehyde peak centered at 550 K. This band is therefore attributable to the presence of vanadium. Both CO and H_2 are detected above 480 K, very likely due to the decomposition of formate species on the surface of the catalyst. This interpretation is supported by the observation of formate species in infrared spectra taken for temperatures above 480 K. It is also noted that H_2O and not H_2 is formed below 550 K, in contrast to the results for TPO, where the H_2 desorption peak occurs at a lower temperature. This may be because most of the surface is covered by methoxide species, which block the zirconia surface sites necessary for readsorption of formaldehyde until higher temperatures. Finally, a large excess of H_2O forms from 575 to 650 K, which coincides with a minimum in oxygen concentration. This peak is likely due to the removal of a large amount of surface species, likely hydroxyl or hydride species that might be present on the surface, since there is no noticeable increase in a carbon-containing species over this same temperature range. Figure 13B is an Arrhenius plot of the formaldehyde formation from 475 to 525 K. The apparent activation energy calculated from the slope of the line is 18 ± 1 kcal/mol, with an apparent pre-exponential factor of 7.0×10^6 $atm^{-1}s^{-1}$.

TABLE 3: Comparison of Loading and Activation Energies for Vanadium Supported on SiO_2, TiO_2, and ZrO_2

	surface area m^2/g	V loading wt %	surface density V/nm^2	E_{app} kcal/mol	ko ($\times 10^6$) atm^{-1} s^{-1}
V/TiO_2	97	1.6	2.0	16	5.3
V/ZrO_2	84	1.9	2.0	18	7.0
V/SiO_2	1370	3.43	0.30	23	23

Comparison of V/ZrO_2 with V/SiO_2 and V/TiO_2. A comparison of the rate parameters for V/ZrO_2 with those for V/SiO_2[10] and V/TiO_2[11] is presented in Table 3. The V surface density of the V/SiO_2 sample is sufficiently low so that all of the dispersed vanadia is present as isolated, tetrahedrally

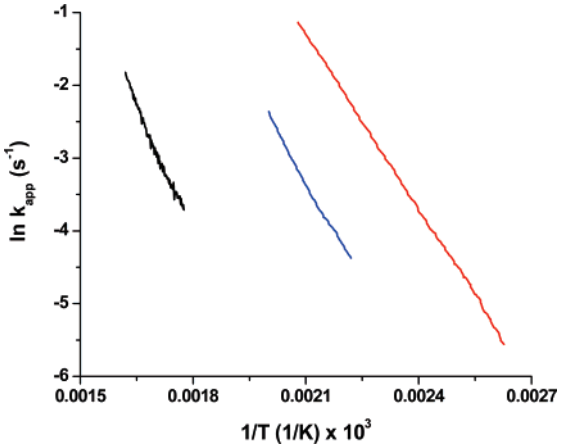

Figure 14. Arrhenius plot comparing the rate of formaldehyde formation during TPRx conditions for V/SiO_2 (black), V/ZrO_2 (blue), and V/TiO_2 (red).

coordinated, vanadate species. At the higher V surface density used for the V/TiO_2 and V/ZrO_2 samples, the dispersed vanadia is present predominately as isolated, tetrahedrally coordinated, vanadate species but a small amount (<10%) may also be present as polyvanadate species.[22] Table 3 shows that the apparent activation energies for formaldehyde formation are nearly the same for V/TiO_2 and V/ZrO_2, 16 and 18 kcal/mol, as are the values of the pre-exponential factors, 5.3×10^6 and 7.0×10^6 $atm^{-1}s^{-1}$, respectively. By contrast, the activation energy and pre-exponential factors for V/SiO_2 are noticeably larger, 23 kcal/mol and 2.3×10^7 $atm^{-1}s^{-1}$, respectively. While the apparent pre-exponential factor for V/SiO_2 is higher than that for V/TiO_2 or V/ZrO_2, the higher apparent activation energy V/SiO_2 contributes to its significantly lower activity, as can be seen in Figure 14.

The results of the present investigation are in qualitative agreement with those reported earlier by Wachs and co-workers, who showed that specific activities of V/ZrO_2 and V/TiO_2 are comparable, and both are nearly 10^3 higher than that of V/SiO_2.[9,23] Wachs and co-workers have proposed that the higher activities of V/TiO_2 and V/ZrO_2 relative to V/SiO_2 are due to the effects of the support on the electronic properties of dispersed vanadate species. In support of this interpretation, they note that the methanol oxidation activity of supported vanadium oxide catalysts increases with decreasing Sanderson electronegativity of the cation in the metal oxide support.[9,22] While this explanation is plausible, the authors do not to show what electronic properties of the supported vanadate species change under conditions for which the structure of the vanadate species is identical on all supports. It is also noted that theoretical calculations of the apparent activation energies for formaldehyde formation on isolated vanadate species supported on silica, titania, and zirconia give nearly identical values, as do more recent calculations carried out with more realistic representations of the support.[24,25] A further observation is that while a change in the electronic properties of the vanadate species might explain the observed difference in apparent activation energy with changes in support composition, it is harder to understand how such support composition could affect the pre-exponential factor for methanol oxidation (see refs 9 and 23), since the vibrational frequencies for $V-OCH_3$ species, the precursor to formaldehyde, are virtually identical for V/SiO_2, V/TiO_2, and V/ZrO_2. Here too, theoretical studies show that the apparent pre-exponential factors should be the same for isolated vanadate species supported on silica, titania, and zirconia.[25]

These considerations lead us to propose that other factors may be responsible for the differences between the rate parameters for V/SiO_2, V/TiO_2, and V/ZrO_2. One possibility is the occurrence of O-atom defects in the oxide support. On the basis of the literature, the surface concentration of defects should decrease in the order $ZrO_2 > TiO_2 \gg SiO_2$.[26−28] Moreover, where bulk O-atom defects can form, such as in the case of TiO_2 and ZrO_2, such defects are known to migrate to the support surface where they could alter the electronic and, hence, catalytic properties of the vanadate species.[29] Preliminary calculations of these effects for V/TiO_2 support this argument.[30] The presence of O-atom defects on the surface of the TiO_2 support would also explain the lower activation energy measured on isolated vanadate species on TiO_2 when compared with previous studies with a monolayer of vanadate species on the surface. The O-atom defects on the surface of the support would be covered by the monolayer of vanadium. However, at a loading of 2.0 V/nm^2, that used in the studies of isolated vanadate species supported on titania,[11] a large portion of the surface remains uncovered and able to accommodate defects.

Conclusions

The interactions of methanol with ZrO_2 and V/ZrO_2 (2 V/nm^2) were investigated by in situ infrared spectroscopy. Methanol dissociatively adsorbs on ZrO_2 to form $Zr-OCH_3/Zr-OH$ pairs. Upon heating the catalyst, a portion of the $Zr-OCH_3/Zr-OH$ pairs recombines to form CH_3OH, and H_2O is formed by the recombination of pairs of Zr−OH groups. At higher temperatures $Zr-OCH_3$ groups react mainly to H_2 and CO, as well as small amounts of DME. Large amounts of hydrogen are detected in the presence of gas-phase oxygen, along with CO, CO_2, and H_2O. The addition of oxygen leads to the formation of a high-temperature water peak, which is likely due to the oxidation of hydrogen. On V/ZrO_2, the predominant species after methanol adsorption are $V-OCH_3/Zr-OH$ pairs, together with small concentrations of $Zr-OCH_3/Zr-OH$ pairs. CH_2O is produced at moderate temperatures during TPRx on V/ZrO_2. This product appears to originate from $V-OCH_3$ groups formed upon the adsorption of CH_3OH. CH_2O is not detected in increased quantities during the TPD and TPO experiments on V/ZrO_2, most likely because of the readsorption of CH_2O onto the zirconia surface to produce a large number of surface formate species and H_2. At higher temperatures, these formate species undergo decomposition to form CO, and in the presence of O_2, these products can be further oxidized to CO_2 and H_2O. The activity of V/ZrO_2 for the formation of CH_2O at 450 K is 8 times lower than V/TiO_2 and 82 times higher than that of V/SiO_2. The methanol oxidation activity of isolated vanadate species supported on different supports correlates inversely with the apparent activation energy of each catalysts: V/TiO_2 (16 kcal/mol) < V/ZrO_2 (18 kcal/mol) < V/SiO_2 (23 kcal/mol). The factors responsible for the change in apparent activation energy were not established in the course of this work but are thought to include changes in the electronic properties of the supported vanadate species caused by differences in the electronic properties of the support, as well as the possible effects of O-atom defects on TiO_2 and ZrO_2.

Acknowledgment. This work was supported by the Director, Office of Energy Research, Office of Basic Energy Sciences, Chemical Science Division, of the U.S. Department of Energy under Contract No. DE-AC02-05CH11231. Portions of this research were carried out at the Stanford Synchrotron Radiation

Laboratory, a national user facility operated by Stanford University on behalf of the U.S. Department of Energy, Office of Basic Energy Sciences.

Supporting Information Available: Infrared spectra from 3000−4000 cm^{-1} during the TPD and TPO experiments. This information is available free of charge via the Internet at http://pubs.acs.org.

References and Notes

(1) Deo, G.; Wachs, I. E. *J. Catal.* **1994**, *146*, 323.
(2) Baltes, M.; Cassiers, K.; van der Voort, P.; Weckhuysen, B. M.; Schoonheydt, R. A.; Vansant, E. F. *J. Catal.* **2001**, *197*, 160.
(3) Lim, S.; Haller, G. L. *Appl. Catal. A* **1999**, *188*, 277.
(4) Olthof, B.; Khodakov, J.; Bell, A. T.; Iglesia, E. *J. Phys. Chem. B* **2000**, *104*, 1516.
(5) Burcham, L. J.; Deo, G.; Gao, X.; Wachs, I. E. *Top. Catal.* **2000**, *11/12*, 85.
(6) Deo, G; Turek, A. M.; Wachs, I. E. *Appl. Catal., A***1992**, *91*, 27.
(7) Dilara, P. A.; Vohs, J. M. *Surf. Sci.* **1994**, *321*, 8.
(8) Narishige, N.; Niwa, M. *Catal. Lett.* **2001**, *71*, 63.
(9) Burcham, L. J.; Wachs, I. E. *Catal. Today* **1999**, *49*, 467.
(10) Bronkema, J.; Bell, A. T. *J. Phys. Chem. C* **2007**, *111*, 420.
(11) Bronkema, J. L.; Leo, D. C.; Bell, A. T. *J. Phys. Chem. C* **2007**, *111*, 14530.
(12) Pokrovski, K. A.; Bell, A. T. *J. Catal.* **2005**, *235*, 368.
(13) Wachs, I. E.; Weckhuysen, B. M. *Appl. Catal., A* **1997**, *157*, 67.
(14) Jentoft, R. E.; Deutsch, S. E.; Gates, B. C. *Rev. Sci. Instrum.* **1996**, *67*, 2111.
(15) Newville, M. *J. Synch. Rad.* **2001**, *8*, 322.
(16) Ravel, B.; Newville, M. *J. Synch. Rad.* **2005**, *12*, 537.
(17) Gao, X.; Fierro, J. L. G.; Wachs, I. E. *Langmuir* **1999**, *15*, 3169.
(18) Wong, J.; Lytle, F. W.; Messmer, R. P.; Maylotte, D. H. *Phys. Rev. B* **1984**, *30*, 5596.
(19) Binet, C.; Daturi, M. *Catal. Today* **2001**, *70*, 155.
(20) Pokrovski, K. A.; Rhodes, M. D.; Bell, A. T. *J. Catal.* **2005**, *235*, 368.
(21) Zhu, J.; van Ommen, J. G.; Lefferts, L. *J. Catal.* **2004**, *225*, 388.
(22) Tian, H. T.; Ross, E. I.; Wachs, I. E. *J. Phys. Chem. B* **2006**, *110*, 9593.
(23) Burcham, L. J.; Badlani, M.; Wachs, I. E. *J. Catal.* **2001**, *203*, 104.
(24) Khaliullin, R. Z.; Bell, A. T. *J. Phys. Chem. B* **2002**, *106*, 7832.
(25) Goodrow, A.; Bell, A. T. *J. Phys. Chem. C* **2007**, *111*, 14753.
(26) Eder, D.; Kramer, R. *Phys. Chem. Chem. Phys.* **2006**, *8*, 4476.
(27) Eder, D.; Kramer, R. *Phys. Chem. Chem. Phys.* **2003**, *5*, 1314.
(28) Imai, H., et al. *Phys. Rev. B* **1988**, *38*, 12772.
(29) Jug, K.; Nair, N. N.; Bredow, T. *Phys. Chem. Chem. Phys.* **2005**, *7*, 2616.
(30) Goodrow, A.; Bell, A. T., unpublished results.